Automated Design and Production of Cranioplasty Plates: Outer Surface Methodology, Accuracies and a Direct Comparison to Manual Techniques

Frederik Gelaude[1], Jos Vander Sloten[1] and Bert Lauwers[1]

[1] Katholieke Universiteit Leuven, frederik.gelaude@mech.kuleuven.be

ABSTRACT

Large vulnerable openings in human cranium require a rigid anatomical reconstruction. A possible solution is the use of personalised thin titanium plates, also denoted membranes. The indirect production process, which is mainly hydroforming or casting, requires a single die, which is shaped manually or milled directly from a CAD-file.
Currently, the design of membranes is mainly manual work, even with the use of CAD facilities, and results in a tedious and user-dependent skull reconstruction. A direct link between CAD-file and production is missing, and no studies evaluate the overall geometrical outcome quantitatively.
This paper therefore presents an innovative automated design-methodology for custom-made cranioplasty plates. For a clinical case, the time durations and shape deviations are assessed and compared with results of the current artisanal design procedure. The afore-mentioned required improvements are achieved.

Keywords: titanium membranes, automated design, CAD, shape comparison.

1. INTRODUCTION

Permanent reconstructions of large vulnerable openings in human cranium, also denoted cranioplasty, can be attained by the use of personalised titanium membranes. First the shape of these preformed sheet metal implants is assessed and then an appropriate production technique is applied [4][8][9][11].
Current shape reconstruction techniques for the skull surface, either with modelling clay and spatulas in a lab, in a layer-by-layer or Boolean CAD approach [7][11], or in a specialised software environment [3Matic®][ProEngineer®] are highly effective but still require much manual input and focus mainly on the design. Fully three-dimensional design approaches have also been investigated – e.g. a rigid piece of bone at the healthy side of the skull is cut out and mirrored to the affected side, or standard shapes such as a hemisphere are applied – but manual after-processing is required to obtain a smooth transition to the surrounding bone and mirroring techniques cannot be applied when the defect extends over both sides of the skull [Mimics®][7].
Current indirect production techniques such as casting [6] and hydroforming [8][11] require a single die which shape is deduced directly from the planned skull reconstruction. These dies are either hand-made or milled [8]. In case of the former, much manual work is spent on creating the dies, additional time for die hardening is needed, and inaccuracies are inevitably introduced in each imprinting stage. At the present time no studies report on the overall die accuracies, on plate accuracies and on the influence of each intermediate step of the production process. Joffe *et al.* assessed only the degree of compliance of the plate on a test skull with a 'feeler gauge' [8], while others judge the shape reconstruction or fit on a qualitative basis [4][9[11].
The application field of personalised surface based implants, such as titanium membranes, or even its alternatives being PMMA reconstructions or bone cutting templates for autografts [5], can be broadened if the clinical outcome is good, if a significant reduction in surgery duration is obtained, and if these implants/tools are rapidly available for a reasonable price. A solution to these requirements includes an efficient and automated design environment which develops personalised implants for multiple types of bone defects, thereby enabling a streamlined production.
On the one hand, this paper therefore presents and applies a newly developed semi-automated surface-based CAD approach to address the above-mentioned *design* problem. A generally developed bone contour filter- and mesh procedure [3] is used to extract only the bony outer surface information from available Computed Tomography (CT) data. Meanwhile, the procedure automatically detects and reconstructs bone defects which may be present in a skull

(cranium). A smooth skull reconstruction plate (cranioplasty plate) can then be extracted directly from the triangulated surface mesh. From this plate, an intelligent hydroforming pressing-die design is created.
On the other hand, this paper addresses the above-mentioned *accuracy assessment* problem by outlining an objective evaluation protocol for the shape of cranioplasty plates. A single clinical cranioplasty-case exemplifies this protocol. The automated approach is directly compared to the (current) artisanal alternative procedure; this encompasses a deviation statistics (closest points distances) between surface scans of the dies and plates.

2. MATERIALS AND METHODS

Firstly, the state-of-the-art of the artisanal procedure to reconstruct cranial defects is presented. The same paragraph is used to outline the current plate forming technique, namely hydroforming, and the plate postprocessing step. Then, the newly developed contour-based CAD approach is addressed.

2.1. Artisanal Plate Design and Production

Once a bone defect is diagnosed and a titanium membrane is chosen as a reconstruction method, a manual design sequence is initiated by acquiring a CT-scan, segmenting the bone from this scan, and producing a physical model of the skull by means of stereolithography (SLA) (fig. 1, left). The segmentation of the skull bone is thereby performed in a commercial 3D image processing and editing software [Mimics®][Medicim®][InVesalius®][Velocity®][Analyze®]; a greyvalue thresholding operation first selects the 'bony' voxels, after which a Marching Cubes algorithm [10] is applied to build a three-dimensional triangulated representation (STL) of the skull.
Subsequently, a technician manually reconstructs the defect region with clay (further designated as 'die1'). After hardening of the clay, a physician outlines the outer contour of the defect and broadens this region, with a considerable overlap region for the reconstruction plate. Then a negative cast is made from the SLA model, with the reconstruction clay in place ('die2'), followed by the production of a positive die in plaster of Paris ('die3'). A positive copy of the latter is made in a metal reinforced epoxy ('die45') by using a negative silicone die. Only the latter is not displayed in fig. 1. Meanwhile, the orientation of the die is manually adjusted; on average the reconstruction region now faces the ground plane, thus facilitating the subsequent hydroforming pressing stage.

SLA (top view) die1 die2 Die3 die45 (hydroforming die)

Fig. 1. Artisanal (manual) design procedure: SLA model and successive cast dies, with their respective number.

Hydroforming, which is the current plate forming technique, requires only one die to press the plate against a rubber membrane, which in turn seals an oil reservoir [8]. A variant to this technique consists in placing a rubber membrane between a hydraulic metallic cylinder and the titanium plate, thus also obliterating the need for a counter die [11]. In this paper the variant is used. The titanium plate is initially between 0.2 and 0.7 mm thick, is circular of shape and has a minimal diameter of 150 mm. When the oil reservoir is pressurised, the rubber membrane bows out, or in our case the metallic cylinder protrudes. Firstly, the plate is clamped at the borders; subsequently the oil pressure is further increased and a first contact is made with the top of the die. The pressure is only gradually increased to prevent wrinkling and tearing; each pressing stage alternates with a membrane trimming and polishing stage. If the membrane does wrinkle, hammering can be applied to recover the membrane, although mostly the process has to be re-initiated with a flat piece of plate, even so in case of membrane tearing. As no direct numerical models on hydroforming of sheet titanium are readily available, the operator determines the machine settings and the number of steps from his experience. Finally, the circular piece of work is transferred to a lab for a post-processing step. The reconstruction region in the plate is cut out, nicely trimmed to the plate border that was outlined by the physician, and further bent manually to certainly fit the SLA model. If wanted, screw insertion holes and perforation holes for the cerebrospinal fluid (CSF) are drilled. The finishing touch then consists in etching and sterilisation, to obtain a clean membrane.

2.2. Automated Plate Design and Production

This paragraph first describes the generally developed methodology to retain only outer bone-contour information from a segmented CT-scan, and to convert this set to a triangulated bone surface mesh. The skull defect in the mesh is thereby automatically detected and reconstructed. The mesh then directly enables the calculation of a smoothed reconstruction plate. Finally, from this plate, a triangulation of a hydroforming die is automatically created.

2.2.1 Bone Contour and Surface Mesh Methodology

Within this research, a general filter and mesh procedure was developed to create outer surface meshes of intact bones, starting from bone contours (fig. 2(a)). These contours are generated by a Marching Squares [10] operation in commercially available CT-image processing software. Since the current paper applies the developed methodology to skull defects in particular, and since full detail (noise, classification of contours as external, etc.) on the developed filter procedure is available elsewhere [3], only the sub-procedures which establish the skull defect reconstruction are envisaged below. More specific, this encompasses the removal of large internal defect loops in the bone contours (fig. 2(b)), spline approximation (fig. 2(c)) and mesh building (fig. 2(d)).

Three categories of internal loops are differentiated, depending on the distance between the start and endpoint of the loops, the percentage of enclosed polyline points, and the global/local property of the loop with respect to the entire contour area. Table 1 gives an overview of this classification.

Loop Variant class	D	A	N [%]
1	restricted	global	15
2	infinite	global	50
3	infinite	local	25

Tab. 1. Parameter settings for the internal loop removal procedure. Three categories of internal loops are defined. ‘D’: distance between start and endpoint of a loop; ‘A’: search area for loops in a contour (global = all contour points may be start or endpoint); ‘N’: number of polyline points present in the loop.

1st Variant loops. If the bone cortex has a small opening in the CT images, a large internal loop is formed in the bone contour. The procedure seeks for nearby start and endpoints, which enclose more than a specific amount of points. The loop is considered internal when one side of its XY-envelope at most, coincides with the XY-envelope of the original contour. In every iteration step, the loop with the largest enclosed area is removed (fig. 3, fig. 2(b)).

Additional to 1st variant loops, wide open U-shaped loops appear in the neurocranium base contours, or when dealing with bone defects. As this information is undesirable for membrane reconstructions, it must be removed from the set. With this in view, two more variations on the procedure that removes internal loops are implemented. They vary the above-described parameters (tab. 1). In contrast to the first variant, the procedure now only removes the largest loop and does not insert interpolation points.

2nd Variant loops. For every segment of the polyline the angle is calculated, using a horizontal axis as a reference. If the range of the least squares lines in the cumulative angle diagram of a contour is small (fig. 4), large internal loops are expected. The loop contains about fifty percent of all points present in the contour (fig. 3). The loop removal procedure is then executed with no distance or position limitation for the points in a pair and is halted after removing the largest loop.

3rd Variant loops. Finally, a third variant is implemented to search open cortices in a constrained search area, without any restriction on the distance between start and endpoints. To define the search area and the contours to investigate, the user either indicates a search region on a three dimensional visualisation mesh of the bone or a fixed search area on the global grid in caudal-cranial view.

Subsequently, periodic least-squares approximating splines are calculated (fig 2(c), fig. 3). The maximum deviation between a specific polyline point and its corresponding spline point is user-defined, and the value is automatically lowered for smaller polylines. A surface mesh is then built from the spline set (fig. 2(d)). A grid of quadrilaterals is created after selecting a fixed number of points on each spline. The optimal correspondence between points of two different layers is thereby calculated by minimizing the least squares sum of the distances between the pairs. The surface mesh is closed at the top contour with a Delaunay [1] based triangulation, and then converted to STL.

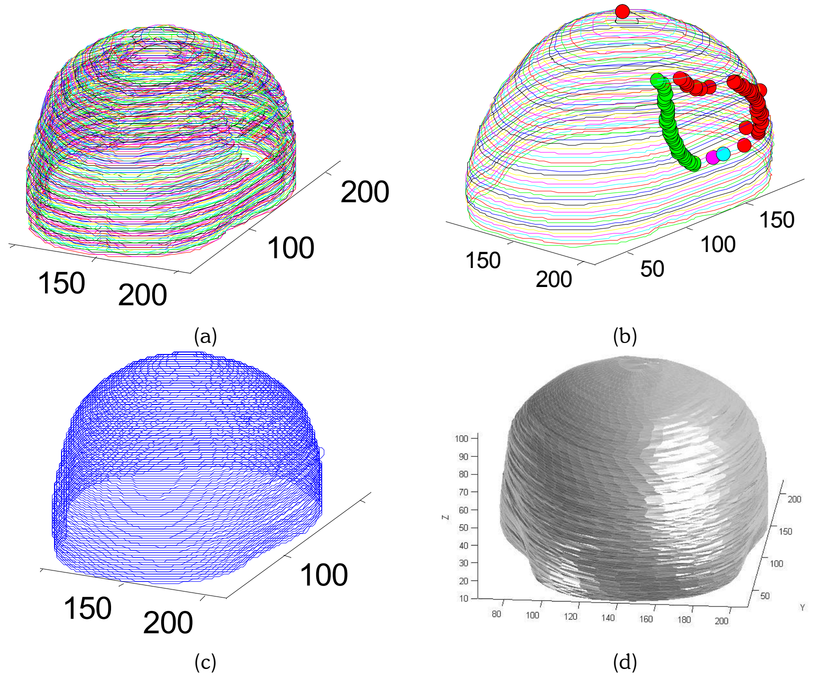

Fig. 2. Bone contour filtering, defect detection and correction: skull defect. Bone contours are extracted from the CT images by a thresholding operation, followed by a Marching Squares operation (a). A filter procedure then retains only outer bone contour information. A loop removal procedure (three variants) automatically detects the defect zone (b), while a spline calculation corrects the missing anatomical curvature (c). From the spline set, a triangulated surface representation is built (d).

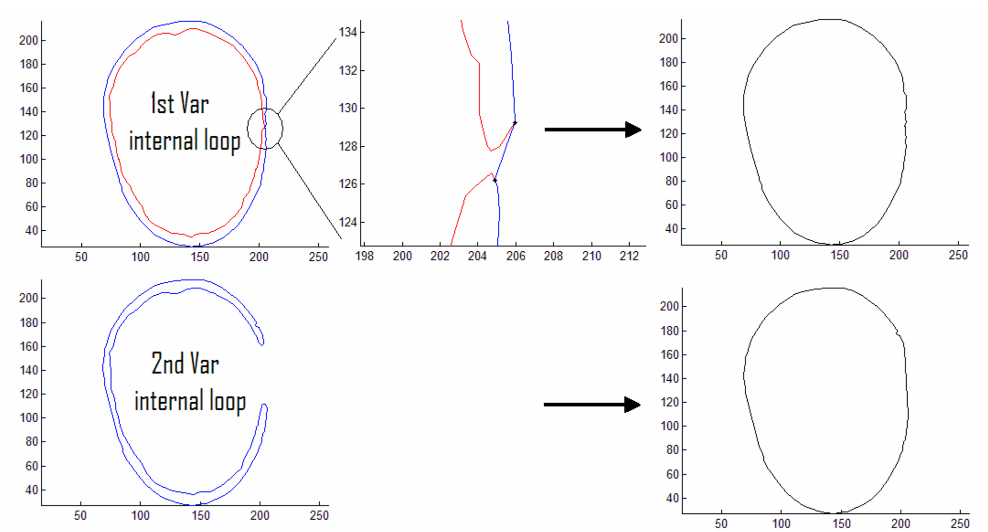

Fig. 3. Detection and correction of internal loops: in-plane (XY) view. The procedure seeks for nearby start and endpoints, which enclose more than a specific amount of points. The defect is then reshaped by a closed spline approximation of the bone contour (right).

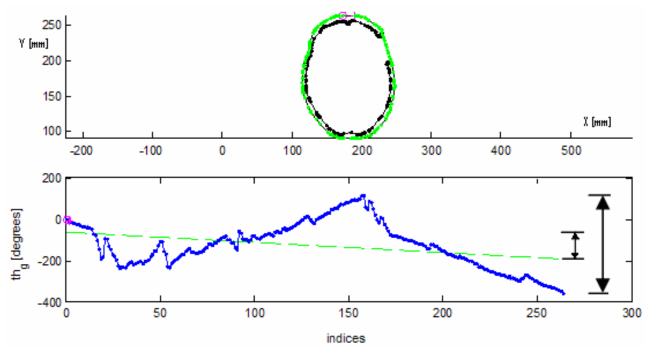

Fig. 4. Detection and removal of large internal loops (second variant). The detection of a large opening in the bone contour is based on the least squares line of the angle VS indices data points, which is plotted as a dotted line. If the range of this line is small with respect to the overall range of the angle diagram, a large internal loop is expected.

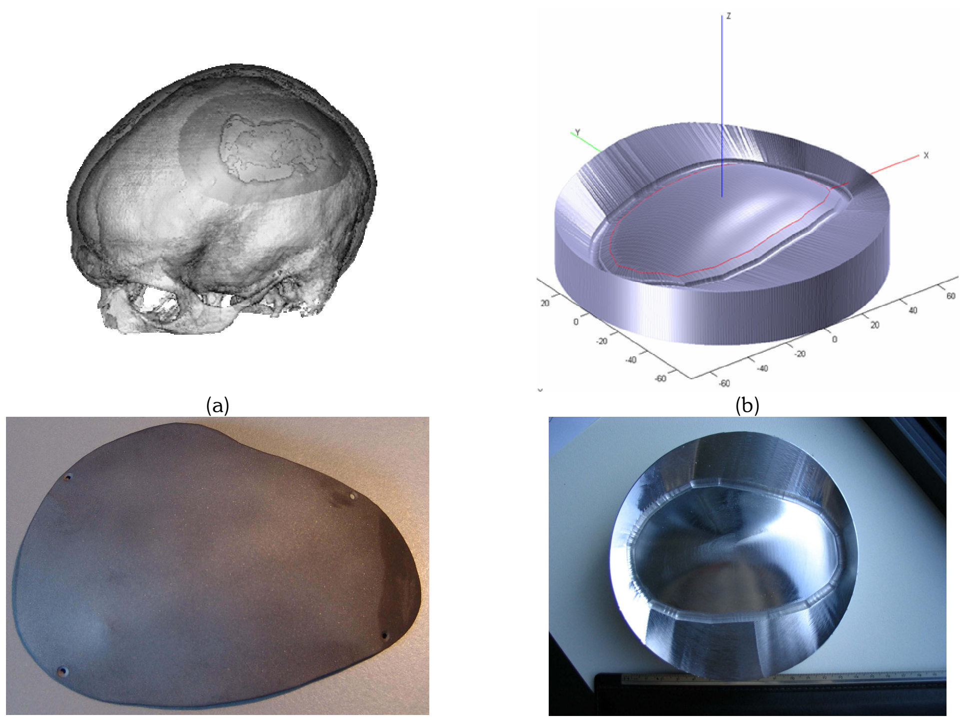

(a) (b) (c) (d)

Fig. 5. Clinical cranioplasty case: plate and die design. Once the defect zone is broadened with an interactively indicated overlap region (a), a smoothing plate is generated (b, central region). The STL representation of the plate is subsequently adapted to obtain a specific die design (b). The personalised titanium membrane (c) is formed, using the milled physical die (d).

2.2.2 Semi-Automated Plate Design

Applying the filter sequence on a contour set with middle-sized hole automatically leads to a reconstruction of the hole since the start and endpoints of the large defect loops are detected by the three above-described ‘variants’ for loop removal, and corrected by spline interpolation (fig. 3, fig. 2(c)). The surface mesh just requires some smoothing in the defect region; no further reconstruction is needed (fig. 2(d)). The region of interest is outlined on the outer surface mesh, which includes an overlap with the sound surrounding bone (fig. 5(a)). A thin plate smoothing spline is then calculated only for the enclosed surface entities. Because this spline approximation requires a functional surface, the mesh region is reoriented. This can be done either by analysing the contour points in the defect region with respect to the main bone axis, or calculating the mean normal of the triangulated defect region. With the mesh region facing the ground plane, the thin plate smoothing spline is calculated for the mesh points present. As this procedure is matrix-based, a rectangular plate is obtained first, but redundant points are easily removed since the plate outline is known. Finally the plate is exported in STL format by triangulating every quadrilateral. This procedure results in the plate in figure 5(b) (central region). A first validation of the plate curvature is assessed by visualising the plate on the CT-data in commercially available imaging software (fig. 6).

2.2.3 Enhancing Plate Production

The trimmed STL plate was used to create a hydroforming die. Figure 5(b) illustrates a possible approach. From the operators' expertise, a narrow trench and a rising collar are included in the die design. During hydroforming the former ensures that the plate finally more easily touches the entire extension region, while the latter realizes a continuous clamping of the plate border during consecutive trimming/forming stages.
The STL files of the plate and the die are the input for a subsequent milling procedure. A milled die (fig. 5(d)) can be used directly for the above-described hydroforming procedure (paragraph 2.1). The plate post-processing is also similar. Finally, a plate as presented in fig. 5(c) is obtained.

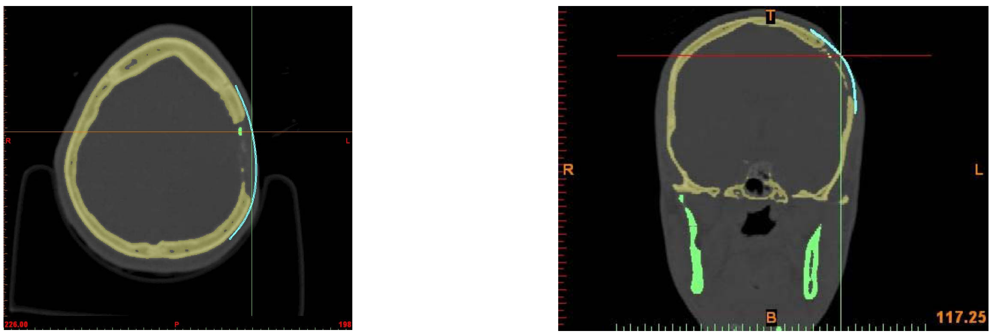

(a) (b)

Fig. 6. Validation of plate curvature on the CT data (in Mimics©). (a) axial view, (b) coronal view.

2.2 Validity of the Automated Design Approach

At present, cranioplasty plate-implants are most commonly judged subjectively, either by the surgeon during operation, or pre-operatively by a technician in a lab. However, to investigate the outcome quality of a new design methodology, a more objective, inter-observer invariable evaluation method is preferred. A comparison protocol is set-up to validate the outcome of the developed automated design methodology. On the one hand the time-durations are measured, while on the other hand the geometrical outcome is judged by using a scanning device. This paragraph further investigates a method to characterise the geometrical outcome.
The shapes of the available dies and plates have been assessed using an optical measuring device (laser stripe scanning, Metris LC 50, Metris N.V., Belgium). This device determines the distances between measuring points on the object and the scan head, and combines it with the 3D-information from a coordinate measuring machine (Mitutoyo FN-905, Mitutoyo Corp., Japan). In case of translucent materials the scanned work pieces are uniformly sprayed with a fine layer of white dust. The accuracy of the measuring system is then between 15 and 35 microns.
Table 2 presents the scanned point sets, and the comparisons that were performed. For each 'comparison' in the table, the point set in the second column is compared with the point set in the third column; the comparison number is mentioned in the first column. First, the measured point clouds were thinned using a grid of size 0.4 mm. Then, the CADcompare software (Metris N.V.) was run to match each couple of point sets (Iterative Closest Point algorithm [2]) and to assess the deviations. The latter is defined as the distances between the closest point pairs.
With this scanning approach, three remarks have to be stated. Firstly, although the translucent SLA model and die1 could both be sprayed, scanned and vapour cleaned, this was not done to ensure that the material remained usable for intra-operative sterile use. Secondly, the membranes were scanned twice, namely once entirely on the inside, and once in clamped position. The latter method does not allow a complete scan of the plates, more specific the most occipital region was not scanned, but this method was required for a correct acquisition of the inside with respect to the outside (thickness). And thirdly, the ICP-matching was logically not applied in case of the thickness assessments of the membranes (comparisons 5 and 6 in table 2).

3. RESULTS

For a single clinical cranioplasty case, both the artisanal and the newly developed CAD design-procedure were applied. A first paragraph describes the time durations of both procedures, while a second paragraph compares the geometrical outcome by means of the above-described surface-scan protocol.

3.1 Procedure Description and Time Durations

3.1.1 Artisanal Design and Production

A CT-scan of a patient with a left temporal-parietal defect in the neurocranium was assessed (fig. 6). After segmentation, the SLA model building required at least 24 hours (fig. 1, left). This SLA model served as starting point for a manual, technician-determined clay reconstruction. Figure 1 shows the consecutive die impressions that were obtained. The hardening of the reinforced die lasted 24 hours, while the other dies together are workable after a couple of hours. Depending on logistics and availability of the hydroforming equipment, a plate is formed on the reinforced die approximately ten days after the design, or later. After an additional two days for plate post-processing, the plate was available for implantation.

A plate with diameter 150 mm and 0.5 mm thickness was hydroformed using the reinforced die45. The post-processing was carried out by fitting the plate on the SLA model.

Diagnosis CT-scan	SLA model	Manual design	Auxiliary dies reorientation	Reinforced die	Hydroforming Plate> clamp> press> trim >	holes etching sterilisation
depends on availability	min. 1 day	2 days	4 hrs	24hrs	1-2 hrs, depending on complexity	2 days
			Approx. min. 10 days			
Hospital	e.g. Materialise	Unident lab	Ceka N.V.			Unident lab

Fig. 6. Artisanal plate design and production: time duration.

3.1.2 Automated Design and Production

Figure 2(a) presents the neurocranium with a left temporal-parietal defect. Starting with 162 bone contours in slices with 1 mm of inter-slice distance, 54 internal and 14 small contours were immediately removed by using previously-developed filter procedures [3]. A single internal loop with nearby start and endpoints was corrected (first variant); this loop contained at least 24 points – out of 300 – with start and endpoint closer than 3.5 mm. Then 43 wide open loops were automatically removed (second variant), clearing all middle-sized loops from the set (fig. 2(b)). During a visual inspection, none of the contours required an adaptation with the provided correction tools.

The default imposed accuracy in one point of the splines (fig. 2(c)) was set to 1mm and automatically lowered for the smaller contours. The mean imposed and obtained accuracies for the splines used for the neurocranium surface mesh are 0.93 ± 0.14 and 0.80 ± 0.17mm respectively. The surface mesh (fig. 2(d), built from fifty points per spline, represents only the exploitable outer hemispheric part of bone surface, contains less noise and nicely covers the defect region. The uncompiled Matlab® program obtained a reconstructed surface mesh in 30 minutes[1], from which about five minutes were used for thresholding and user interactions.

After indicating a broad membrane region on the surface mesh, a thin plate smoothing spline was calculated. The anatomical temporal-parietal curvature was nicely traceable in the STL representation of the reconstruction plate.

The STL membrane was further trimmed in close correspondence to the three-dimensional visualisation and the patients CT data (fig. 6). The latter also indicates that the fit of the membrane on the skull is good; the transition between reconstruction and overlap region is smooth. In total, the entire acquisition, filter, mesh building, membrane generation, refinement and validation lasted about 45 minutes, mainly mere calculation time. An additional five minutes were needed to automatically create a hydroforming die from the trimmed plate. An aluminium hydroforming

[1] Calculation time using a Celeron® 2.0 GHz processor, with 512Mb of internal memory, uncompiled Matlab® code.

die was three-axis milled in 210 minutes, from which only one man-hour was required for initializing the CAM procedure. A plate with diameter 150 mm and 0.5 mm thickness was hydroformed in ten minutes, more specific in three stages, alternated with a single hammering and trimming stage. The post-processing was carried out by fitting the plate on the aluminium die.

3.2 Geometrical Outcome: Automated CAD VS. Artisanal

Table 2 presents the deviation statistics for the proposed point sets, while figure 7 illustrates the spread of the acquired deviations. Following conclusions can be drawn from these data:

- (comparisons 1-2-3): Since a membrane is only between 0.2 and 0.7mm thick, it can be concluded that the successive manual die imprinting steps separately introduce a relatively high inaccuracy. Nevertheless, the summed accuracy of consecutive positive and negative impressions is better (fig. 7(a)).
- (comparison 4): The automatically designed aluminium die was milled with a mean accuracy of 0.01 mm. The transfer of the planning (STL-file of the die) to a physical die by means of milling is thus more accurate than the application of successive imprinting steps. The deviation range of this comparison would become even smaller if trench and collar points were excluded from the point sets.
- (comparisons 5-6): The membrane thickness of the automatically shaped milled aluminium die is more uniform. This can clearly be concluded from the histogram of the deviations in fig. 7(b).
- (comparison 7): The manually shaped membrane is wavier, though this is not anatomically required (fig. 7(c)). Moreover, the automatically shaped membrane contains anatomically correct smooth curvatures. Analysis of the matched plate positions indicates that the automatically shaped membrane covers a different skull region, which suggests that a partly different region was manually cut out from the hydroformed plate in the post-processing stage.
- (comparison 8): The aluminium was only deformed slightly. No similar comparison information was available for the manually shaped die.
- (comparisons 9-10): The plate springback of the manually designed plate is not negligible with respect to the other comparison results, even taken into account that the plate was bent by a technician in a lab (fig. 7(d)). A comparison of the automatically shaped plate could not be performed because the matching of the datasets was not unambiguous.

No.	… VS. …		Focus on:	Max. [mm]	Mean ± sdev [mm]
1.	die2A	die3A	Casting accuracy	5.711	0.532 ± 0.510
2.	die3A	die45A	Casting accuracy	2.886	0.896 ± 0.221
3.	die2A	die45A	Casting accuracy	5.553	0.357 ± 0.458
4.	die B, STL	die B, unused	3-axis Milling	1.568	0.009 ± 0.146
5.	membrane A, outside	membrane A, inside	Thickness	0.677	0.491 ± 0.050
6.	membrane B, outside	membrane B, inside	Thickness	1.231	0.497 ± 0.034
7.	membrane A, inside	membrane B, inside	Shape design	3.050	0.438 ± 0.339
8.	die B, unused	die B used	Die deformation	1.441	0.318 ± 0.072
9.	die45A, used	membrane A, inside	Finishing	4.907	0.528 ± 0.527
10.	die B used	membrane B, inside	Finishing	-	-

Tab. 2. Calculated comparisons of scanned point sets. Deviations are defined as the distances between closest point pairs of two point sets. (A= artisanal design, B= automated design).

4. DISCUSSION

A contour-based reconstruction method for neurocranium defects was presented. A bone contour set with middle-sized defect is automatically reconstructed by applying a general filter sequence [3]. The resulting surface mesh just requires some smoothing in the defect region; no further reconstruction is needed. With the presented methodology, defects up to one third of the skulls' perimeter can be treated. The adopted layer-by-layer approach proves effective in reconstructing three-dimensional defects. Moreover, a fluent transition between original and reconstructed skull regions is guaranteed. This fluent transition is a major advantage compared to procedures which use Boolean operations of volume STLs [7]. Moreover, if compared to (reverse-)engineering software packages (PRO-engineer, 3Matic, AutoCad) [11], the presented CAD approach is more automated, cancelling out user dependencies. User interaction is restricted to important decision-taking steps only.

From the reconstructed surface mesh, a smoothed reconstruction plate can be deduced directly, and automatically

converted into a pressing die with favourable design features. Since the die contains uniform extension, trench and collar regions, the hydroforming procedure became more straight-forward; the number of pressing cycles were decreased. Further research will address the fine-tuning of the die by means of numerical analysis and testing.
The post-processing of the plate should be enhanced by cutting the hydroformed plate more exactly on the planned outline. The plate outline, which is numerically available in the automated approach, can for example be used in an wire-EDM procedure (Electrical Discharge Machining), thereby using reference points as a positioning aid.
Currenlty, the shape of custom-made titanium plate implants is mostly judged in a subjective and qualitative way [4][9][11]. To assess the validity of the presented procedure objectively, the time durations were tracked and the geometrical outcome was investigated. As an example, a single cranioplasty case illustrated the design and validation methodology; the results were compared to the artisanal alternative.
The geometry analysis indicates that, for the presented simulation case, the automated plate design was faster, less user-dependent, and resulted in a plate with more uniform thickness. The overall accuracy is at least comparable to the artisanal procedure; the plate is moreover smooth and nonetheless anatomically more correct.
For the illustrated case, the developed automated reconstruction methodology delivered a plate and die design in less than fifty minutes, mainly mere calculation time. The entire design and die production procedure lasted $4^{1/2}$ days and 260 minutes (one day) for the artisanal and automated approach respectively. The artisanal approach required five dies and a rather expensive SLA model (>1000EUR).
Future work will consistently apply the presented design and curvature validation methodology on new cases, which will enable us to generalize the presented results.

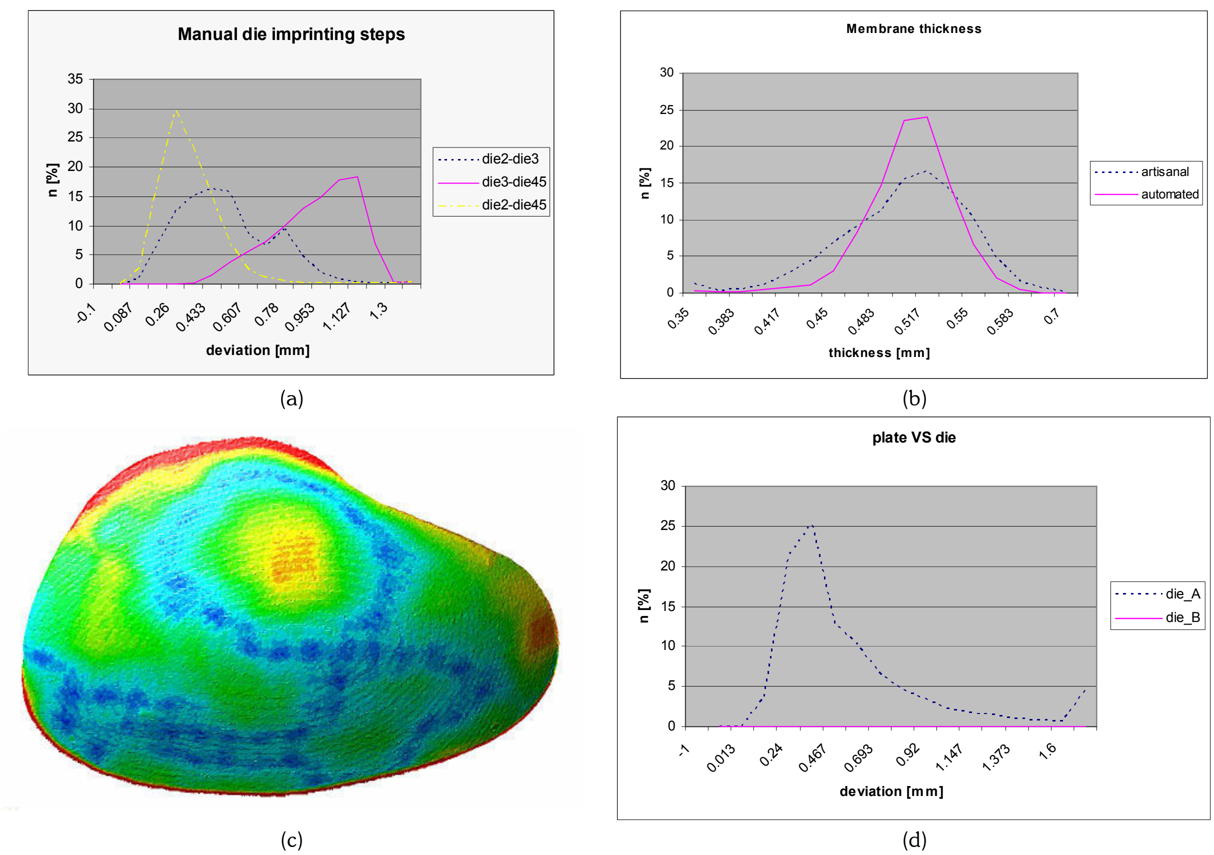

Fig. 7. Comparison results. (A= artisanal design, B= automated design) (a) Casting dies 2, 3 and 45 of the artisanal design method. (b) Membrane thicknesses (c) Membrane A inside compared to membrane B inside (d) Finishing step.

5. CONCLUSIONS

Enhanced preoperative computer-assisted implant-design enables reduction of design and production time durations, and more user-independent bone defect reconstructions. Well-designed personalised implants may in turn lower the operation duration. The developed general filter and mesh procedure proves effective in automatically reconstructing craniofacial defects and extracting a surface based implant design, and facilitates subsequent implementations such as automated hydroforming die design.

6. ACKNOWLEDGEMENTS

We would like to express our gratitude to Dr. Dumans (Erasmus MC, Rotterdam, The Netherlands) for providing the CT data of the cranial bone defect, to the Materialise company, for putting at disposal the Mimics® 3D image processing and editing software, and to ir. Pierre Lefebrve (K.U.Leuven), Vincent De Buck (Ceka N.V). and Ludovic Beckers (Unident N.V.) for their feedback on the automated die design. This research is funded by a Ph.D grant of the Institute for the Promotion of Innovation through Science and Technology in Flanders (IWT-Vlaanderen).

7. REFERENCES

[1] Barber, C., Dobkin, D. and Huhdanpaa, H., The Quickhull Algorithm for Convex Hulls, *ACM Transactions on Mathematical Software*, Vol. 22, No. 4, 1996, pp 469-483.

[2] Besl, P. J. and McKay, N. D., A method for registration of 3D shapes, *IEEE PAMI*, Vol. 14, No. 2, 1992, pp 239-256.

[3] Gelaude, F., Vander Sloten, J. and Lauwers, B., Semi-automated segmentation and visualisation of outer bone cortex from medical images, *accepted for CMBBE.*

[4] Connell, H. M., Statham, P. F., Collie, D. A., Walker, F. S. and Moos, K. F., Use of a template for custom cranioplasty, *Phidias Newsletter*, No. 2, June 1999.

[5] Hayward, R. D., Cranioplasty: don't forget the patient's own bone is cheaper than titanium, *British Journal of Neurosurgery,* Vol. 13, No. 5, 1999, pp 490-491.

[6] Heissler, E., Fischer, F.-S., Bolouri, S., Lehmann, T., Mathar, W., Gebhardt, A., Lanksch, W. and Bier, J., Custom-made cast titanium implants produced with CAD/CAM for the reconstruction of cranium defects, *Int. J. Oral Maxillofac. Surg.*, Vol. 27, 1998, pp 334-338.

[7] Hieu, L. C., Bohez, E., Vander Sloten, J., Vatcharaporn, E., Binh, P.H., An, P.V. and Oris, P, , Design for medical rapid prototyping of cranioplasty implant, *Rapid Prototyping Journal*, Vol. 9, No. 3, 2003, pp 175-186.

[8] Joffe, J. M., Nicoll, S. R., Richards, R., Linney, A. D. and Harris, M., Validation of computer-assisted manufacture of titanium plates for cranioplasty, *Int. J. Oral Maxillofac. Surg.,* Vol. 28, 1999, pp 309-313.

[9] Koppel, D. A., Moos, K. F. and Walker, F. S., Skull reconstruction with a two-part interlocking custom-made titanium plate, *British Journal of Oral and Maxillofacial Surgery,* Vol. 37, 1999, pp 70-72.

[10] Lorensen, W. E. and Cline, H. E., Marching Cubes: A High Resolution 3D Surface Construction Algorithm. *Computer Graphics*, Vol. 21, No. 4, 1987, pp 163-169.

[11] Pattijn, V., Samson, I., Vander Sloten, J., Van Audekercke, R., Swaelens, B., and De Buck, V., Medical image based, preformed titanium membranes for bone reconstructions: design study and first clinical evaluation, *Proceedings of the institution of mechanical engineers, part H - Journal of Engineering in Medicine*, Vol. 216, 2002, pp 13-21.